High-field magnetization of $S=1$ antiferromagnetic bond-alternating chain compounds

Yasuo Narumi* and Koichi Kindo
KYOKUGEN, Osaka University, Toyonaka, Osaka 560-8531, Japan

Masayuki Hagiwara
RIKEN(The Institute of Physical and Chemical Research), Wako, Saitama 351-0198, Japan

Hiroki Nakano
Graduate School of Science, Himeji Institute of Technology, Kamigori, Ako, Hyogo 678-1297, Japan

Akira Kawaguchi
NTT Basic Research Laboratories, Atsugi, Kanagawa 243-0198, Japan

Kouichi Okunishi
Faculty of Science, Niigata University, Niigata, Niigata 950-2181, Japan

Masanori Kohno
Computational Materials Science Center, National Institute for Materials Science, Tsukuba 305-0047, Japan
(Received 3 September 2003; revised manuscript received 24 February 2004; published 6 May 2004)

High-field magnetization and susceptibility measurements have been performed on $S=1$ antiferromagnetic bond-alternating chain compounds: $[Ni_2(dpt)_2(\mu\text{-}ox)(\mu\text{-}N_3)](PF_6)$ [dpt=bis(3-aminopropyl)amine, ox=C_2O_4] (abbreviated as NDOAP) and $[Ni(333\text{-}tet)(\mu\text{-}NO_2)]ClO_4$ [333-tet=*N*,*N*′-bis(3-aminopropyl)-1,3-propanediamine] (abbreviated as NTENP). The magnetization of NDOAP shows two steep increases at about 200 and 500 kOe. A magnetization plateau is observed between about 300 and 500 kOe, corresponding to half the value of the saturation moment. Comparison between numerical calculations and the experimental results, including the magnetic susceptibility, shows that NDOAP has a singlet ground state due to dimerization with a bond-alternating ratio $\alpha=0.1$. The half-saturation plateau is also observed around 700 kOe in the magnetization of NTENP. The magnetization process of NTENP is well reproduced by the numerical result calculated for the parameter of $\alpha=0.45$ in the singlet-dimer phase. The α dependence of the magnetization processes is discussed.

DOI: 10.1103/PhysRevB.69.174405 PACS number(s): 75.10.Jm, 75.50.Ee

I. INTRODUCTION

In the past 20 years, several theoretical predictions for low-dimensional quantum spin chains have been verified by experimental studies. In particular, a large part of them were triggered by Haldane's conjecture in 1983,[1,2] which states that an energy gap exists for the Heisenberg antiferromagnetic chain with integer spin values, while there is no gap for the chain with half-integer spins. Thereafter, his argument has been applied to more complicated and generalized quantum spin systems.

Affleck and Haldane have described the Heisenberg antiferromagnet with bond alternation (HABA) by the Hamiltonian

$$\mathcal{H}=\sum_i [1+(-1)^i\delta]\boldsymbol{S}_i\cdot\boldsymbol{S}_{i+1}, \tag{1}$$

where δ represents the strength of the bond alternation and S_i is the $S=1$ spin operator at site i.[3–6] They have shown that the system has massless critical points only at $\theta=(2k+1)\pi$ with $k=0,\pm1,\pm2,\ldots$, where θ is the topological angle given by $\theta=2\pi S(1-\delta)$ based on the O(3) nonlinear σ model. This means that a HABA with spin S is expected to have $2S$ quantum critical points with gapless excitation. In addition to this, recently the condition for gap formation in a high magnetic field has also been presented, which can be also viewed as a kind of generalization of the Haldane conjecture.[7] The magnetization m of a quantum spin chain is topologically quantized as

$$n(S-m)=\text{integer}, \tag{2}$$

where n is the period of the ground state. This expression is particularly important in the analysis of a HABA with explicit periodicity $n=2$, implying that the magnetization curve of a HABA with $S\geqslant1$ may exhibit characteristic plateaus.

Among the various possible HABA's, the one with $S=1$ has got particular experimental interest since some of these compounds have actually been synthesized. Theoretically, the following results are predicted for the HABA with $S=1$. Depending on the value of δ, two different ground states with an energy gap are possible: the singlet-dimer phase and the Haldane phase, which can be connected with an isolated dimer gap with $\delta=1$ and with the original Haldane's conjecture with $\delta=0$, respectively. At the phase boundary, the energy gap vanishes with a massless excitation. For the gapless point, Singh and Gelfand[8] have applied

a series-expansion technique and have estimated the critical value to be $\delta_c = 0.25 \pm 0.03$. Several numerical studies supporting this estimated value for δ_c have been performed by using the density-matrix renormalization-group (DMRG) method[9] and the quantum Monte Carlo (QMC) method.[10] For the HABA in a magnetic field, theoretical studies have shown that, for $\delta \neq 0$, the magnetization may be quantized at $m = 1/2$, in addition to $m = 0$ and 1.[11]

As discussed above, the magnetic behavior of the HABA with $S = 1$ is theoretically rather well predicted. The question arises which material is suitable to verify experimentally the behavior of a HABA with $S = 1$. In the experimental studies of $S = 1$ spin systems, the most important compounds are the ones consisting of Ni(II) ions. In fact, several Ni(II) chain compounds with alternating bonds have been synthesized.[12–16] These compounds have two different types of bridging ligands or two crystallographically different ligands which connect Ni^{2+} ions, resulting in the formation of $S = 1$ chain structures with bond alternation. However, the studies performed on these compounds mainly concern the relation between the magnetic interactions and the chemical bonds and not much attention has been paid to properties such as the gap formation, the gapless point, and the magnetization plateau.[3–7,11,17]

The aim of the present work is to carry out a systematic experimental study of the HABA, enabling a comparison with theoretical predictions. For this purpose, a series of HABA compounds is needed with typical bond-alternating parameters δ in a variety of the Ni based compounds. The gapless point has previously been confirmed by magnetization and susceptibility measurements on the HABA compound $[Ni(333\text{-tet})(\mu\text{-}N_3)](ClO_4)$ [333-tet=*N*,*N*′-bis(3-aminopropyl)-1,3-propanediamine] (abbreviated as NTEAP).[18] It also has been shown that the ground state of $[Ni(Medpt)_2(\mu\text{-ox})(\mu\text{-}N_3)]\ (ClO_4)\cdot 0.5H_2O$ [Medpt =methyl-bis(3-aminopropyl)amine] (abbreviated as NMOAP) ($ox = C_2O_4$) lies in the singlet-dimer phase and that its magnetization process has a half-saturation plateau.[19] In order to study the HABA systematically as a continuous function of δ, other HABA compounds that fill in the region of missing δ values are required.

In this paper, we report on experiments on two types of Ni^{2+} chain compounds $[Ni_2(dpt)_2(\mu\text{-ox})\ (\mu\text{-}N_3)](PF_6)$ [dpt = bis(3-aminopropyl)amine, ox = C_2O_4] (Ref. 14) (abbreviated as NDOAP) and $[Ni(333\text{-tet})(\mu\text{-}NO_2)](ClO_4)$ (Ref. 15) (abbreviated as NTENP). Magnetization and susceptibility measurements have been performed on these two compounds and the obtained results are compared with numerical calculations by means of the exact diagonalization method[20] and the DMRG method.[21–25] Finally, we present the experimentally determined magnetic phase diagram for HABA (Fig. 8).

The paper is organized as follows. In the following section, details of sample preparation and the experimental equipment are presented. Section III is devoted to the crystal structures of NDOAP and NTENP. In Sec. IV, we report the experimental results and compare them with the numerical calculations. In Sec. V, we compare the alternating exchange interactions with the bridging ligands and discuss the magnetization plateau in the quantum spin system. The experimental results are summarized in a three-dimensional display as function of the magnetization, of the magnetic field, and of the bond-alternating ratio. In the final section, the results are summarized.

II. EXPERIMENTAL PROCEDURES

Single-crystalline samples were synthesized by a slow-evaporation method. Here, we present the preparation procedure of NTENP. The compound NDOAP was synthesized in a similar way. Stoichiometric amounts of $Ni(ClO_4)_2\cdot 6H_2O$ (purity 99.99%) and 333-tet amine were mixed in ultrapure water and the aqueous solution was filtered. Then, an aqueous solution of the required stoichiometric amount of $NaNO_2$ was added to the filtrate and the solution was put on a shelf for about 1 month.

The temperature dependence of the magnetic susceptibility was measured in a SQUID (Superconducting QUantum Interference Device) magnetometer (Quantum Design MPMS-XL7L). Diamagnetic corrections were carried out according to Pascal's sum rule of the diamagnetic contributions from chemical bonds and the elements of the compound.[26] High-field magnetization measurements were performed by using pulse magnets that can produce magnetic fields up to 800 kOe without destruction. The magnets have been made by winding coils of Cu-Ag wire. The coils are reinforced by a ring of Maraging steel with a tensile strength exceeding 200 kgf/mm^2. The magnets are immersed in liquid nitrogen in order to lower the electrical resistance and to reduce the Joule heat. Field pulses of about 550 kOe can be generated every 25 min. Experimental data are collected by utilizing a digital transient memory IWATSU DM-2350. The values of the magnetic field and the magnetization were calibrated by the spin-flop transition field and the linear increase after the transition in the magnetization curve of the typical antiferromagnet MnF_2.

III. CRYSTAL STRUCTURES

A. NDOAP

$[Ni_2(dpt)_2(\mu\text{-ox})(\mu\text{-}N_3)]\ (PF_6)$ (NDOAP) crystallizes in the monoclinic structure, space group $P2_1/a$ with the lattice parameters $a = 10.989$ Å, $b = 19.357$ Å, $c = 12.598$ Å, and $\beta = 107.27°$.[14] Figure 1(a) shows the molecular structure. It is noted that the counteranions PF_6^- are omitted for simplicity. Each Ni^{2+} ion is coordinated octahedrally by three nitrogen atoms of an aminate ligand, by two oxygen atoms of an oxalato ligand, and by one nitrogen atom of an azido ligand. These Ni^{2+} ions are linked to both neighboring Ni^{2+} ions by the oxalato and the azide ligands, respectively. Consequently, the Ni^{2+} ion chains are composed of alternating bridges along the *a* axis.

B. NTENP

$[Ni(333\text{-tet})(\mu\text{-}NO_2)](ClO_4)$ (NTENP) crystallizes in the triclinic structure, space group $P\bar{1}$.[15] The lattice constants and angles at room temperature are $a = 10.747(3)$ Å, *b*

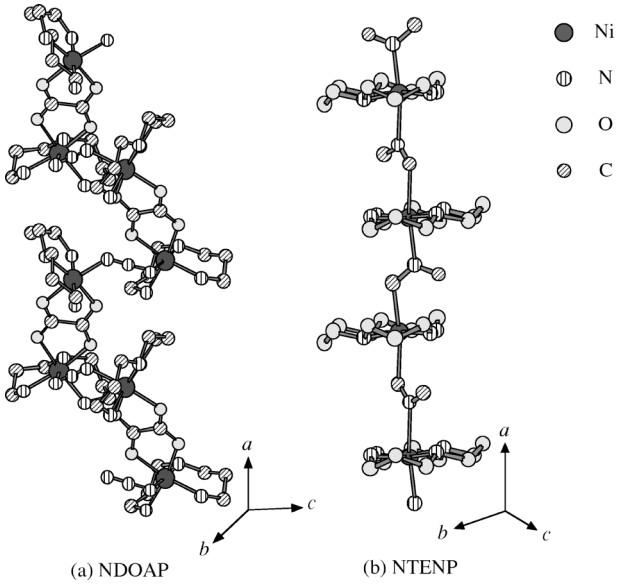

(a) NDOAP (b) NTENP

FIG. 1. Chain structures of NDOAP (a) and NTENP (b). The counteranions PF_6^- for NDOAP, ClO_4^- for NTENP, and hydrogen atoms for both compounds are omitted for simplicity. Each atom is represented by different circles as illustrated in the figure.

$=9.413(2)$ Å, $c=8.789(2)$ Å, $\alpha=95.52(2)°$, $\beta=108.98(3)°$, and $\gamma=106.83(3)°$.[15] Figure 1(b) shows the chain structure of NTENP. The chain is composed of Ni^{2+} ions bridging through nitrito groups. The nitrito groups are disordered as is common in these kinds of compounds. Each chain is well isolated by ClO_4^- counteranions with which no hydrogen bonds exist. The most important feature is that the inversion centers are not situated on the Ni^{2+} ions but on the nitrito groups and two different bond distances of 2.142(3) Å and 2.432(6) Å exist between the Ni^{2+} ions. As a result, this compound is expected to be of the bond-alternating chain type.

IV. RESULTS AND ANALYSES

A. NDOAP

1. Susceptibilities

The magnetic susceptibility of NDOAP is shown in Fig. 2. The magnetic field is applied along the *a*, *b*, and *c** axes, where the *c** axis is defined to be perpendicular to the *a* and *b* axes. The susceptibilities along the different axes are almost identical. The susceptibility has a broad maximum at about 40 K. In the low-temperature region, the susceptibility steeply decreases to almost zero, indicating the existence of an excitation gap above the singlet ground state. For the *a* axis, the maximum value is 2.5% smaller than for the other axes which is due to a slightly smaller *g* value for the *a* axis than for the other axes.

We compare the susceptibility along the *a* axis with the numerical calculations in terms of the exact diagonalization method.[20] Defining the *a* axis, which is the chain direction, as the magnetic principal *z* axis, we consider the Hamiltonian

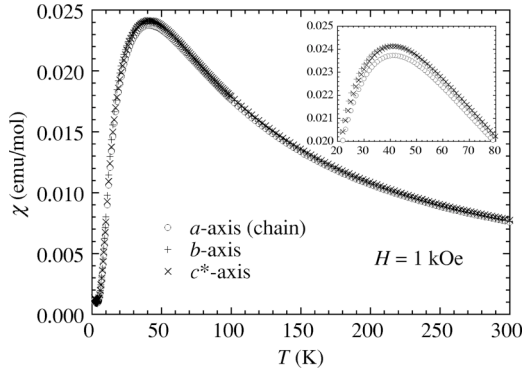

FIG. 2. Temperature dependence of the magnetic susceptibility of NDOAP in a magnetic field of 1 kOe. The susceptibility around the broad maximum is shown in the inset. The open circles, pluses, and crosses represent the experimental data obtained with the field applied along the *a*, *b*, and *c** axes, respectively.

$$\mathcal{H}=J\sum_{i=1}^{N/2}(\boldsymbol{S}_{2i-1}\cdot\boldsymbol{S}_{2i}+\alpha\boldsymbol{S}_{2i}\cdot\boldsymbol{S}_{2i+1})-\sum_{i=1}^{N}g_z\mu_B S_i^z H_z, \tag{3}$$

where N is the system size number, J and αJ are the exchange constants between two different nearest neighbors, α is the bond-alternating ratio between two exchange constants mentioned above, g_z is the g value of the Ni ions along the z axis, μ_B is the Bohr magneton, S_i^z is the z component of $\boldsymbol{S}_i$, and H_z is the applied magnetic field along the z axis. For the ratio α, it holds that $\alpha=(1-\delta)/(1+\delta)$. Note that the critical point $\delta_c\cong 0.25$ corresponds to $\alpha_c\cong 0.6$. In the following sections, α will mainly be used to identify bond-alternating chain compounds. In the calculations, periodic boundary conditions have been imposed and the system size has been taken up to eight sites.

The experimental χ_{expt} curve has been fitted by the calculated χ_{calc} curves. Figure 3 shows the fitting result for various values of α. The curve obtained for a bond-alternating ratio $\alpha=0.1$ reproduces χ_{expt} quite well and the obtained parameters are $J/k_B=40.1$ K and $g_z=2.23$ for the *a* axis.

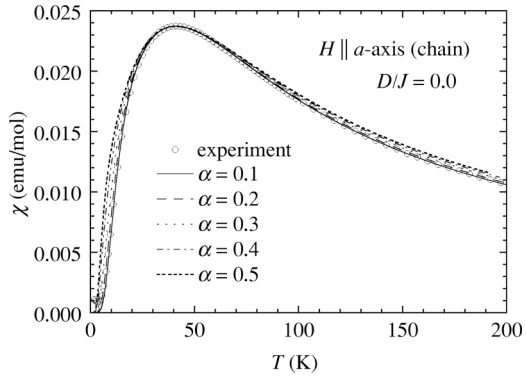

FIG. 3. Temperature dependence of the magnetic susceptibility of NDOAP, calculated for different values of the bond-alternating ratio α by means of the exact diagonalization method with $J/k_B=40.1$ K, $g_z=2.23$. The open circles represent the experimental data of NDOAP along the *a* axis.

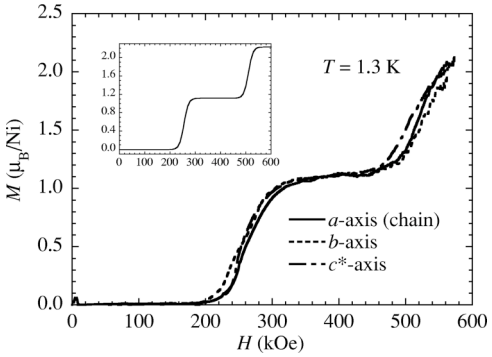

FIG. 4. Magnetization curves of NDOAP at 1.3 K along the *a* (solid line), *b* (dotted line), and c^* axes (dashed and dotted line). Each magnetization has been normalized to that along the *a* axis at the half-saturation plateau. The inset shows the magnetization curve calculated for an $S=1$ antiferromagnetic isolated dimer with the parameters $T=1.3$ K, $g=2.23$, and $J/k_B=38.2$ K obtained from the fit in Fig. 5.

These parameters are in satisfactory agreement with the values of $J/k_B=39.4$ K, $\alpha=0.1$, and $g=2.19$, which have been derived from the susceptibility of a powdered sample.[14]

2. Magnetizations

High-field magnetization measurements were performed at 1.3 K in fields up to about 600 kOe, applied along the *a*, *b*, and c^* axes (Fig. 4). Because no hysteresis is observed within the experimental accuracy, only the curves measured with increasing field are shown. Being almost zero in the low-field region, the magnetization increases sharply at about 200 kOe for all directions and reaches half of the saturation value. At about 500 kOe, the magnetization increases again and tends to saturate at about 600 kOe. Similar to the magnetic susceptibility, no clear axial dependence of the magnetization is observed.

The steplike increase of the magnetization clearly indicates the existence of an excitation gap. One of the striking features is the half-saturation plateau observed between about 300 kOe and 500 kOe. The width of the plateau is smaller than that obtained with the isolated dimer model shown in the inset of Fig. 4. This difference arises from the many-body effect of the quantum system, which causes the gradual increase of the magnetization between 200 and 300 kOe and between 500 and 600 kOe.

The magnetization of the bond-alternating chain has also been calculated by means of the exact diagonalization method. Figure 5 shows the curves calculated for $\alpha=0.1$, together with the experimental result along the *a* axis. The calculated result for $T/J=0.00$ deviates from the experimental result around both edges of the gradual slopes of the magnetization. The calculated curve is in better agreement with the experiment, if one takes the thermal effect into account. Using the *g* value obtained from the susceptibility measurement, we get the parameter $J/k_B=38.2$ K which is close to the value derived from the susceptibility measurements.

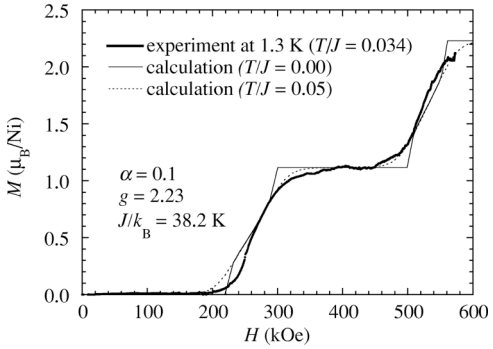

FIG. 5. Magnetization curves of NDOAP for $T/J=0.00$ and 0.05, calculated by means of the exact diagonalization method. The thick solid curve represents the experimental data along the *a* axis.

B. NTENP

1. Susceptibilities and magnetizations below 250 kOe

The susceptibility and magnetization curves shown in Fig. 6 have been reported previously by some of the present authors.[27] The susceptibility curve is compared with the susceptibility calculated numerically by means of the QMC method, giving the parameters $\alpha=0.45$,$J/k_B=54.2$ K, $D/J=0.25$, and $g_z=2.14$ for the magnetic field parallel to the chain direction. In this calculation, a uniaxial single-ion anisotropy term $\Sigma_{i=1}^{N} D(S_i^z)^2$ was introduced into the Hamiltonian (3). The magnetization curves clearly indicate the existence of a gap and the singlet ground state is realized up to around 100 kOe, where the magnetization increases abruptly.

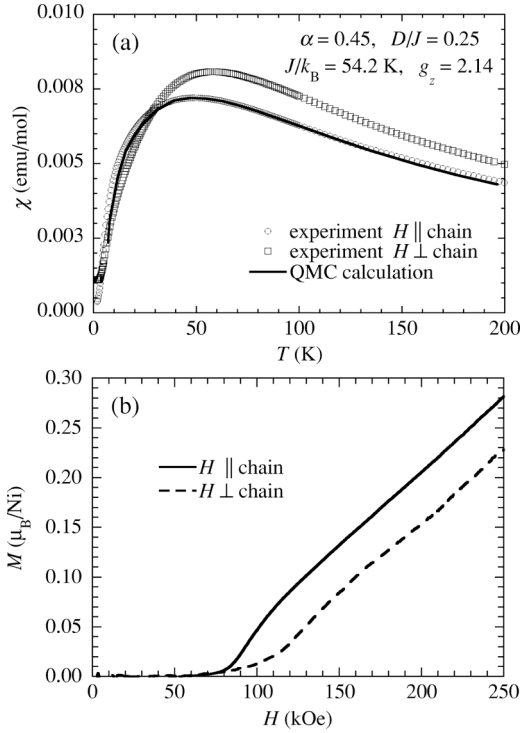

FIG. 6. (a) Temperature dependence of the susceptibility of NTENP at 1 kOe and the susceptibility calculated by means of the QMC method with the parameters shown in the figure. (b) Magnetization curves at 1.3 K up to 250 kOe.

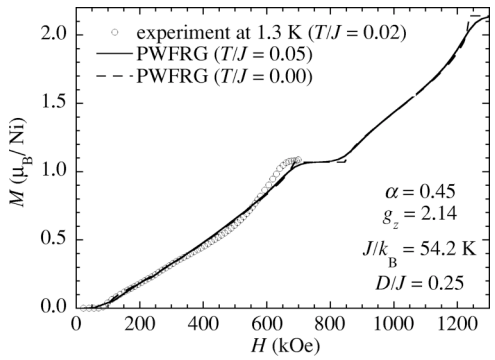

FIG. 7. High-field magnetization process of NTENP up to 700 kOe in the chain direction and the theoretical curves calculated by means of the PWFRG method for $\alpha=0.45$ and $D/J=0.25$ at $T/J=0.00$ and 0.05.

The ground state of NTENP was also verified to be the singlet-dimer phase by the observation of an edge state in NTENP doped with the nonmagnetic impurity Zn.[27]

2. Magnetization up to 700 kOe

Our theoretical calculation suggests that, for the Hamiltonian with the above parameters, the system should have the magnetization half-saturation plateau in a magnetic field higher than 250 kOe. In order to examine this, magnetization measurements up to 700 kOe were performed using the pulse magnet introduced in the preceding section. Figure 7 shows the experimental result together with the calculated curves.

When the magnetic field is applied along the chain, the onset of the half-saturation plateau around 700 kOe can be observed. This experimental result is compared with the theoretical curves for $\alpha=0.45$ and $D/J=0.25$ at $T/J=0.00$ and 0.05, which were calculated by means of the product-wave-function renormalization-group (PWFRG) method[21,22] and by the finite temperature DMRG method,[23–25] respectively. The parameters in the calculations have originally been estimated by Narumi *et al.*[27] Although the experimental curve deviates slightly from the calculated ones above about 400 kOe, the agreement is reasonable.

V. DISCUSSION

A. Bond alternation and chemical bridge

Two exchange constants ($J/k_B=38.2$ K and $\alpha J/k_B=3.82$ K) correspond to the two different superexchange interactions in NDOAP. The compound $[Ni_2(Medpt)_2(\mu\text{-ox})(\mu\text{-}N_3)](ClO_4)\cdot 0.5H_2O$ (abbreviated as NMOAP), which has a similar structure, has the same bridging ligands. The magnetic properties and the α value estimated for this compound have been reported earlier.[19] In Table I, we present the exchange interaction constants of both compounds for comparison.

The correlation between magnetic interactions and bridging ligands have been studied quite well.[13,14,16] The oxalato ligand generally takes a planar conformation, so that there is no significant difference in bond distance and bridging angle among nickel compounds with oxalato bridge. Although there is a little deviation depending on the distance and the angle, the exchange interaction constant was found to be in the range from 55 K to 30 K. On the other hand, since the azido ligand has a great flexibility in bond angle and distance, the exchange interaction through the ligand is expected to be sensitive to these parameters. According to such discussion, we conclude that the oxalato and the azido bridge in NDOAP should contribute to the larger and the smaller values of these alternating interaction constants, respectively.

TABLE I. Alternating exchange interaction constants of NDOAP and NMOAP estimated from the susceptibility and the magnetization measurements.

Compound	J/k_B	$\alpha J/k_B$
NDOAP	38–40 K	4 K
NMOAP	43–44 K	11–13 K

B. Magnetization plateau

Magnetization plateaus have been observed in several kinds of magnetic materials. When a system is strongly anisotropic, for example, $CoCl_2\cdot 2H_2O$,[28] well known as an Ising spin system, magnetization plateaus appear due to spin rearrangement, for instance, from up-down–up-down to up-up–down-up. In addition, antiferromagnets composed of a small number of spins may have plateaus as a result of level crossing of discrete energy levels due to the quantum origin. However, the origin of the magnetization plateau of a HABA is completely different from the above cases because this system is nearly isotropic and the system size is infinite.

Let us first consider an assembly of isolated dimers as a simple quantum case. This corresponds to the case of $\alpha=0$ in the Hamiltonian in Eq. (3). At zero magnetic field, the energy-level scheme consists of a singlet, a triplet, and a quintet state. On application of a magnetic field, level crossing between the singlet and the triplet state and between the triplet and the quintet state will take place. As a consequence, plateaus appear at magnetization per site $m=0$, 1/2, and 1. What happens when the dimers interact weakly with each other so that the system forms a chain? As the interdimer interaction develops, the discrete energy levels spread. The energy gap between the levels may vanish, finally resulting in the formation of an energy band. This does not seem in favor of the occurrence of a magnetization plateau, but it is not trivial whether the plateau vanishes or not. Tonegawa *et al.*[11] have calculated the phase diagram in the magnetic field versus bond-alternating ratio plane by using the exact diagonalization method. They conclude that the half-saturation plateau appears if $D/J\geqslant 0$ and $\alpha\neq 1$. Later, Totsuka[17] investigated the magnetization plateau using the bosonization technique and came to the same result as Tonegawa *et al.*

When we apply the necessary condition for the magnetization plateaus given in Eq. (2) to the $S=1$ HABA, the magnetization is possibly quantized at $m=1/2$, in addition to $m=0$ and 1, as observed in the present experiments. It

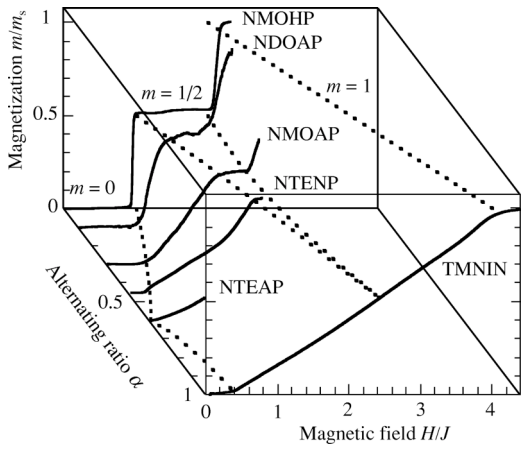

FIG. 8. Magnetization curves of bond-alternating chain compounds in a three-dimensional display of the magnetization, the magnetic field, and the bond-alternating ratio. The dimer compound NMOHP and the uniform chain compound TMNIN are the extreme cases of the bond-alternating chain. The magnetization and the magnetic field are normalized to the saturation magnetization and the strongest nearest-neighbor exchange constant, respectively. The dotted lines represent the phase boundaries without anisotropy as calculated by Tonegawa *et al.* (Ref. 11).

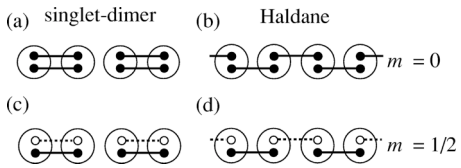

FIG. 9. Schematic representations based on the VBS picture. The small circles represent the spin-1/2 variables. The large open circles show the symmetrization of two spin-1/2 variables to make spin-1 at each site. The solid small circles connected by the solid lines and the open small circles connected by the dotted lines represent the singlet and the triplet pairs, respectively. The details of each sketch are described in the text.

should be noted that the plateau does not always appear when the quantization condition is satisfied. The absence of the plateau with $m=0$ at the gapless point of the HABA is such a case. Note also that the period of the ground state is determined not only by the explicit spatial structure of the Hamiltonian but also by spontaneous symmetry breaking. Such examples are known for the $S=1/2$ case[29] and the $S=1$ case.[30]

C. Phase diagram

Finally, we present the magnetization curves, obtained in the present and in previous works, in a three-dimensional diagram of the magnetization m, the magnetic field H, and the bond-alternating ratio α in Fig. 8. The dotted lines illustrate the phase boundaries with $D/J=0$ calculated by Tonegawa *et al.*[11] For each compound, an estimation of the magnitude of D/J was giving the values $D/J\sim 0$ for NDOAP and NTEAP, 0.07 for NMOAP, and 0.25 for NTENP. There is no qualitative difference in the calculated phase diagram in the H versus α plane in the range of $D/J=0\sim 0.25$. Thus, it seems reasonable to make a comparison between the experimental results and the phase diagram calculated with $D/J=0$.

The magnetization curve of $[Ni_2(Medpt)_2(\mu\text{-ox})\times(H_2O)_2](ClO_4)_2\cdot 2H_2O$ (abbreviated as NMOHP) (Ref. 31) is plotted as a typical curve of the isolated dimer ($\alpha=0$). Large plateaus with $m=0$ and $m=1/2$ were observed like a staircase. On the other side of the bond-alternating ratio ($\alpha=1$), zero magnetization up to $0.41J$ is followed by a continuous increase up to the saturation in the magnetization curve of $(CH_3)_4NNi(NO_2)_3$ (abbreviated as TMNIN).[32] In the intermediate region ($0<\alpha<1$), the magnetization processes of NDOAP, NMOAP,[19] NTENP, and NTEAP (Ref. 18) reproduce the α dependences of the $m=0$ and 1/2 regions. According to the theoretical prediction, as the alternating ratio increases, the spin gap decreases, then vanishes and opens again. On the other hand, the half-saturation plateau survives until the system becomes completely uniform. All experimental results up to now support the prediction concerning the plateau. Unfortunately, no candidate compounds showing the half-saturation plateau have been found so far for the case of $0.6<\alpha<1$.

The schematic representation based on the valence-bond-solid (VBS) (Ref. 33) picture is useful to classify each phase of the HABA. The singlet-dimer ground state consists of two singlet bonds in coupled pairs of spin-1 as shown in Fig. 9(a). On the other hand, the Haldane state consists of singlet bonds of the two spins at one site with the spins at different neighboring sites, as shown in Fig. 9(b). When the phase transition occurs from the Haldane to the singlet-dimer phase at $\alpha=0.6$, a rearrangement of the singlet bonds takes place. The VBS representation has been shown to be valid for the experimental study of NENP, which was the original Haldane chain with $\alpha=1$,[34] and of NTENP, whose ground state was verified to be in the singlet-dimer phase.[27] Upon application of a magnetic field above a critical value, singlet bonds begin to break, making excited triplet pairs, which correspond to the development of the magnetization. When just half of the singlet bonds are broken, the system is in the half-saturation plateau phase. On applying a magnetic field to the system in the singlet-dimer phase, one of two singlet bonds in each coupled spin-1 dimer is broken to produce an excited triplet as shown in Fig. 9(c). On the other hand, for the case of the system in the Haldane phase at zero field, the singlet states which are formed through the weaker exchange interactions change into the excited triplets as shown in Fig. 9(d). We cannot distinguish these two situations, because the excited triplets are likely to move owing to the existence of the intrachain interactions. Thus, we see in the phase diagram that the half-saturation plateau state is a unique phase, independent of α in the $S=1$ HABA.

VI. SUMMARY

We have investigated the $S=1$ antiferromagnetic bond-alternating chain by means of susceptibility and high-field

magnetization measurements on the Ni chain compounds NDOAP and NTENP. Comparison between the experimental results and the numerical calculations leads to the conclusion that NDOAP and NTENP both possess the singlet-dimer ground state with $\alpha \sim 0.1$ and 0.45, respectively. The origin of the bond alternation has been discussed on the basis of the structure. A magnetization plateau at half the saturation magnetization was observed in the magnetization of both compounds. The phase diagram of the HABA in an applied magnetic field was experimentally examined.

ACKNOWLEDGMENTS

This study was partially supported by the Grant-in-Aid for Scientific Research from the Japanese Ministry of Education, Science, Sports, Culture and Technology, and the Molecular Ensemble research program from RIKEN. Most experiments were carried out within the visiting Researcher Program of KYOKUGEN, Osaka University. Thanks are due to Professor F. de Boer for reading the draft and for valuable comments.

*Electronic address: narumi@mag.rcem.osaka-u.ac.jp

[1] F.D.M. Haldane, Phys. Lett. **93A**, 464 (1983).
[2] F.D.M. Haldane, Phys. Rev. Lett. **50**, 1153 (1983).
[3] I. Affleck, Phys. Rev. Lett. **54**, 966 (1985).
[4] I. Affleck, Nucl. Phys. B **257**, 397 (1985).
[5] I. Affleck, Nucl. Phys. B **265**, 409 (1986).
[6] I. Affleck and F.D.M. Haldane, Phys. Rev. B **36**, 5291 (1987).
[7] M. Oshikawa, M. Yamanaka, and I. Affleck, Phys. Rev. Lett. **78**, 1984 (1997).
[8] R.R.P. Singh and M.P. Gelfand, Phys. Rev. Lett. **61**, 2133 (1988).
[9] Y. Kato and A. Tanaka, J. Phys. Soc. Jpn. **63**, 1277 (1994).
[10] M. Kohno, M. Takahashi, and M. Hagiwara, Phys. Rev. B **57**, 1046 (1998).
[11] T. Tonegawa, T. Nakao, and M. Kaburagi, J. Phys. Soc. Jpn. **65**, 3317 (1996).
[12] J.J. Borrás-Almenar, E. Coronado, J. Curely, and R. Georges, Inorg. Chem. **34**, 2699 (1995).
[13] A. Escuer, R. Vicente, J. Ribas, M.S.E. Fallah, X. Solans, and M. Font-Bardía, Inorg. Chem. **33**, 1842 (1994).
[14] A. Escuer, R. Vicente, X. Solans, and M. Font-Bardía, Inorg. Chem. **33**, 6007 (1994).
[15] A. Escuer, R. Vicente, and X. Solans, J. Chem. Soc. Dalton Trans. **1997**, 531 (1997).
[16] A. Escuer, R. Vicente, J. Ribas, J. Jaud, and B. Raynaud, Inorg. Chim. Acta **216**, 139 (1994).
[17] K. Totsuka, Phys. Lett. A **228**, 103 (1997).
[18] M. Hagiwara, Y. Narumi, K. Kindo, M. Kohno, H. Nakano, R. Sato, and M. Takahashi, Phys. Rev. Lett. **80**, 1312 (1998).
[19] Y. Narumi, M. Hagiwara, R. Sato, K. Kindo, H. Nakano, and M. Takahashi, Physica B **246-247**, 509 (1998).
[20] H. Nakano, M. Hagiwara, T. Chihara, and M. Takahashi, J. Phys. Soc. Jpn. **66**, 2997 (1997).
[21] T. Nishino and K. Okunishi, J. Phys. Soc. Jpn. **64**, 4085 (1995).
[22] R. Sato and Y. Akutsu, J. Phys. Soc. Jpn. **65**, 1885 (1996).
[23] X. Wang and T. Xiang, Phys. Rev. B **56**, 5061 (1999).
[24] N. Shibata, J. Phys. Soc. Jpn. **66**, 2221 (1999).
[25] K. Okunishi, Phys. Rev. B **60**, 4043 (1999).
[26] P.W. Selwood, *Magnetochemistry*, 2nd ed. (Interscience, New York, 1956), p. 78.
[27] Y. Narumi, M. Hagiwara, M. Kohno, and K. Kindo, Phys. Rev. Lett. **86**, 324 (2001).
[28] M. Date and M. Motokawa, Phys. Rev. Lett. **16**, 1111 (1966).
[29] T. Tonegawa, T. Nishida, and M. Kaburagi, Physica B **246-247**, 368 (1998).
[30] H. Nakano and M. Takahashi, J. Phys. Soc. Jpn. **67**, 1126 (1998).
[31] Y. Narumi, R. Sato, K. Kindo, and M. Hagiwara, J. Magn. Magn. Mater. **177-181**, 685 (1998).
[32] T. Takeuchi, H. Hori, T. Yoshida, A. Yamagishi, K. Katsumata, J.-P. Renard, V. Gadet, M. Verdaguer, and M. Date, J. Phys. Soc. Jpn. **61**, 3262 (1992).
[33] I. Affleck, T. Kennedy, E.H. Lieb, and H. Tasaki, Phys. Rev. Lett. **59**, 799 (1987).
[34] M. Hagiwara, K. Katsumata, I. Affleck, B.I. Halperin, and J.P. Renard, Phys. Rev. Lett. **65**, 1990 (1990).